Solar Phys (2011) 270:551–559
DOI 10.1007/s11207-011-9762-1

Quadrupolar Dimmings During a Partial Halo Coronal Mass Ejection Event

J. Yang · Y. Jiang · R. Zheng · J. Hong · Y. Bi · L. Yang

Received: 28 October 2010 / Accepted: 28 March 2011 / Published online: 29 April 2011
© Springer Science+Business Media B.V. 2011

Abstract We present detailed observations of the formations of four distinct coronal dimmings during a flare of 17 September 2002, which was followed by an eruption of a huge coronal loop system, and then an over-and-out partial halo coronal mass ejection (CME), with the same direction as the loop system eruption but laterally far offset from the flare site. Among the four dimmings, two compact ones were symmetrically located in the opposite polarity regions immediately adjacent to the highly sheared magnetic polarity inversion line in the flare region, and hence were probably composed of bipolar double dimmings due to a flux-rope eruption and represented its evacuated footpoints. However, another nearby compact dimming and a remote diffuse one were formed in the opposite polarity footpoint regions of the eruptive loop system, and thus probably consisted of a pair of dimmings magnetically linked by the erupting loop system and also indicated its evacuated footpoints. The loop system might have played a role in guiding the erupting flare field and producing the over-and-out CME, but its eruption might simply have been pushed out by the erupting flare field, because there was no reconnection signature between them. From comparison with a derived potential-field source-surface (PFSS) magnetic configuration, our observations consistently suggest that the dimmings were formed in pairs and originated from the eruptions of the two different magnetic systems. We thus define them as "quadrupolar dimmings."

Keywords Corona, activity · Coronal mass ejections, low coronal signatures · Magnetic fields, corona · Prominences, activity

J. Yang · Y. Jiang (✉) · R. Zheng · J. Hong · Y. Bi · L. Yang
National Astronomical Observatories/Yunnan Astronomical Observatory, Chinese Academy of Sciences, P.O. Box 110, Kunming 650011, China
e-mail: yjy@ynao.ac.cn

Y. Jiang
e-mail: jyc@ynao.ac.cn

R. Zheng · J. Hong · Y. Bi · L. Yang
Graduate School of Chinese Academy of Sciences, Beijing 100049, China

1. Introduction

As a key on-disk proxy of coronal mass ejections (CMEs) that represent large-scale reorganizations of the coronal magnetic field, coronal dimmings may have varied forms and have received considerable attention (Hudson and Cliver, 2001). It has become increasingly clear that the configuration of dimmings may reflect the structure of the large-scale magnetic field involved in CMEs (for a review see van Driel-Gesztelyi *et al.*, 2008). Bipolar double dimmings (BDDs), a pair of compact and symmetric dimmings formed in the opposite polarity regions immediately adjacent to the two ends of an eruptive filament or sigmoidal structure, have been explained as the evacuated feet of a large-scale flux rope ejection in some CME events (Sterling and Hudson, 1997; Webb *et al.*, 2000; Jiang *et al.*, 2007). On the other hand, remote brightenings and dimmings, significantly distant from the CME source region, were suggested to be caused by the interaction or reconnection between the expanding twisted flare loops and the overlying large-scale loops (Manoharan *et al.*, 1996; Liu *et al.*, 2006). Jiang *et al.* (2009a) further showed that during a sympathetic CME event, four distinct dimmings were formed in pairs near the opposite polarity footpoints of two different magnetic systems by the interaction between them, a situation that they defined as "quadrupolar dimmings." In particular, Moore and Sterling (2007) also suggested in their magnetic-arch-blowout scenario that remote dimmings can be produced by the blowout of a large quasi-potential magnetic arch caused by a small-scale eruption from its one foot, which can then lead to an over-and-out CME laterally far offset from the initial eruption region (also see Harrison, 1986). In these cases, only few putatively magnetic-loop systems, whether small or large scale in size, participate in the CME eruptions and dimming formations. However, some powerful CME events associated with major flares can involve eruptions of several magnetic flux systems distributed on a large spatial scale (Wang *et al.*, 2002; Chertok and Grechnev, 2005; Zhukov and Veselovsky, 2007), and widespread diffuse dimmings might be produced by reconnection between the erupting field and the surrounding structures (Attrill *et al.*, 2007; Mandrini *et al.*, 2007) or by intercoupling and interaction of multiple flux-loop systems (Delannée, Hochedez, and Aulanier, 2007; Zhang *et al.*, 2007). In this case, it is difficult to identify the one-to-one magnetic connectivity between dimmings in a single event.

Therefore, the relationship between coronal dimmings and large-scale magnetic configuration needs further clarification. We expect that the associated magnetic configuration in some CME events is so simple that we can get clear manifestations of magnetic linkage between dimmings, which will be helpful in understanding their generation mechanism. On 17 September 2002, a partial halo CME was observed by the Large Angle and Spectrometric Coronagraph (LASCO) aboard the *Solar and Heliospheric Observatory* (SOHO). It resulted from a flare of X-ray class C8.6 occurring in active region (AR) NOAA 10114 (S13°W37°) and associated with four distinct coronal dimmings, including three compact ones near the flare site and a remote, diffuse one far away from the flare region. This is an opportunity to investigate in detail the magnetic connectivity between the dimmings. In this paper we will present observations of the dimming formation and comparisons with the coronal magnetic field configuration computed by using the Schrijver and DeRosa (2003) version of the potential-field source-surface (PFSS) model.

2. Observations

The flare was partially covered by observations at Yunnan Astronomical Observatory (YNAO), one station of the global Hα network (Steinegger *et al.*, 2000), which provided

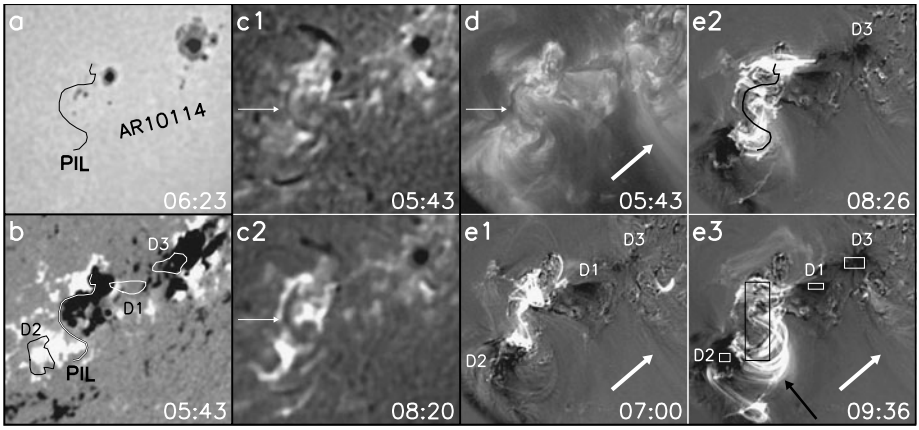

Figure 1 MDI intensity image (a) and magnetogram (b), YNAO Hα (c1 – c2), TRACE 195 Å direct (d), and fixed-base difference (e1 – e3) images, which are obtained by subtracting the 05:43 UT pre-flare direct image. D1, D2, and D3 mark the three compact dimmings, and their outlines determined from the 08:26 UT difference image are superimposed as white and black contours in (b). The polarity inversion line, PIL, determined from the 05:43 UT magnetogram is plotted as black curves in (a) and (e2). The white thin arrows indicate the filament along PIL, the white thick arrows indicate the leg-like feature, and the black arrow indicates the post-flare loops spanning PIL. The solid boxes mark the areas in which Hα and 195 Å light curves are measured and displayed in Figure 3. The FOV is $390'' \times 360''$.

full-disk Hα line-center images with a pixel size of about $1''$ and a 1-min cadence. The most complete observations covering the flare were made by the *Transition Region and Coronal Explorer* (TRACE) (Handy *et al.*, 1999), which provided EUV 195 Å images with a pixel size of $0.5''$ and a 1-min cadence. TRACE's limited field of view (FOV) was centered on the flare core and covered the three compact dimmings well; the remote dimming can only be seen in full-disk EUV images from the Extreme Ultraviolet Imaging Telescope (EIT; Delaboudinière *et al.*, 1995) on SOHO. EIT provided 12-min cadence 195 Å images with a pixel resolution of $2.6''$, while 171, 284, and 304 Å images were taken only once in 6 h. The resulting CME and the magnetic field settings in the associated regions were examined using SOHO/LASCO C2 and C3 data (Brueckner *et al.*, 1995), CME height-time data available at the LASCO web site, low corona white-light observations (1.08 to 2.85 $R_{\odot}$) from the Mark IV K-coronameter (MK4) at the Mauna Loa Solar Observatory (MLSO), and full-disk magnetograms with a pixel size of $2''$ from the Michelson Doppler Imager (MDI; Scherrer *et al.*, 1995) on SOHO. We used *Geostationary Operational Environmental Satellite* (GOES) soft X-ray light curves to track the flare time profile.

3. Results

The flare occurred in the following end of AR 10114 and had start, peak, and end times at around 06:11, 08:20, and 09:36 UT, respectively. Figure 1 shows the general appearances of the region as an MDI continuum intensity image and a magnetogram, and the flare process in YNAO Hα and TRACE 195 Å observations. The region consisted of two main negative polarity sunspots, and the flare was along the magnetic polarity inversion line (PIL) at its eastern boundary. PIL showed a strongly curved profile and a meandering filament laid over

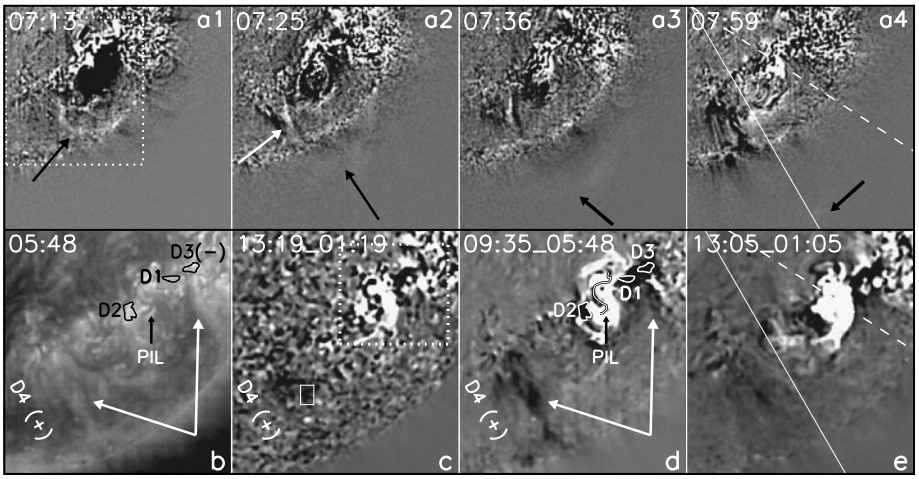

Figure 2 EIT 195 Å running difference images (a1 – a4) showing the erupting huge EUV loop system (black arrows) and its disturbed southeast footpoint (white arrow). EIT 195 Å direct (b), and 304 (c), 195 (d), and 284 Å (e) fixed-base difference images showing the remote dimming, D4, and the two leg-like features corresponding to the footpoint regions of the eruptive loop system (white arrows in (b) and (d)). The dashed lines indicate the PIL radial direction, and the solid lines the final CME direction. The plus signs mark the corresponding positive magnetic polarity in the photosphere. The outlines of D1 – D3 and PIL are also plotted as in Figure 1. The FOVs for (a1 – a4) and (b – e) are $1360'' \times 1340''$ and $820'' \times 880''$, respectively. The dotted boxes in (a1) and (c) indicate the FOVs of (b – e) and of Figure 1, respectively. The solid box marks the measured area of D4 light curves.

it before the flare (indicated by the thin white arrows in Figures 1(c1) and 1(d)), indicating a highly sheared magnetic configuration. The flare showed some features of a two-ribbon flare, such as two Hα ribbons residing on the opposite sides of PIL (see Figure 1(c2)), separation of the two ribbons away from PIL (Figures 1(e1) – (e3)), and the appearance of post-flare loops connecting the ribbons (indicated by the black arrow in Figure 1(e3)). However, the filament did not erupt. At the flare maximum, it is still clearly seen (indicated by the arrow in Figure 1(c2)). A similar example of a two-ribbon flare without involvement of filament eruption was also reported by Wang *et al.* (2004). Quite likely, as a portion of a complex flux-rope system, the filament was lying at a low altitude so that the post-flare loops formed by magnetic reconnection due to an upper eruption of the flux rope could have prevented it from disruption (Pevtsov, 2002). A notable characteristic of the event is the three compact dimmings, D1, D2, and D3, forming around the flare in the TRACE FOV (see Figures 1(e1) – (e3)). D1 and D2 appeared in the opposite polarity regions immediately close to the two ends of PIL, so they probably composed a pair of BDDs. D3 was formed to the northwest of D1 in a negative polarity region and was well distinguished from D1. Since it was coincident with the footpoint region of a bright EUV leg-like feature (indicated by the thick white arrow in Figure 1(d)), which was disturbed in the course of the flare (see the white arrows in Figures 1(e1) and (e3)), we expect D3 to be associated with an expansion of a larger-scale loop system and to have an opposite polarity counterpart in a larger FOV.

EIT observations indeed revealed an eruption of a huge EUV loop system overlying the flare region. In the EIT 195 Å running difference images shown in Figure 2, this eruption manifested itself as an expanding faint semicircular bright rim during the flare (see the black

arrows in Figures 2(a1) – (a4)), along with a strong disturbance at its southeast footpoint (see the white arrow). The footpoint regions of the eruptive loop system appeared as two bright leg-like features in an EIT 195 Å image before the flare (see the two white arrows in Figure 2(b)), and the western one corresponded to that seen in the TRACE images (Figure 1(d)). After the eruption, a remote diffuse dimming, D4, about 0.44 $R_{\odot}$ distant from the centroid of PIL, actually appeared in its positive polarity footpoint region, which is clearly discernible in the EIT fixed-base difference images at 304, 195, and 284 Å (Figures 2(c) – (e)) and showed similar location and shape. Note that in these base difference images D1 and D3 were merged into a larger one due to the lower resolution of EIT images relative to TRACE observations. The fact that D3 was located near the negative polarity footpoint of the loop system (see Figures 1 and 2(b)) makes it very likely that D3, D4 also consisted of a pair of dimmings as a result of the expansion or even opening of the eruptive loop system, and so represented its evacuated feet. This case was very similar to that given by Manoharan *et al.* (1996), but there was a difference in that no persistent brightening was found around D4 during the loop eruption, and no new EUV loop connection developed between the flare core and D4. Therefore, it appears that in our event the loop system was simply pushed out by the highly sheared flare core field without participation of large-scale magnetic reconnection between them.

The associated partial halo CME appeared as a wide loop front and had a width of 249° and a central position angle (PA) of 210°. In Figure 2, the final CME direction determined from the central PA is plotted as solid lines, and the radial direction of PIL, defined as a straight line connecting its centroid to the center of the solar disk, is plotted as dashed lines. We see that the CME direction was laterally far offset from the flare region but nearly along that of the loop system. Although MLSO/MK4 white-light images on the previous day and LASCO observations definitely showed that the CME was not associated with a helmet-streamer structure, noting that the flare was close to the western foot of the eruptive loop system, it can be classified as an over-and-out one according to the definition of Moore and Sterling (2007), and the situation of D4 was very similar to that of the remote dimming in their example. Therefore, we can further speculate that, besides a simple expansion, the loop system might also play a role in laterally channeling the flare eruption and in leading to a 27° deflection of the CME direction from the PIL radial direction (Moore and Sterling, 2007; Jiang *et al.*, 2009b). In Figure 3, the light curves of Hα and TRACE 195 Å intensities of the flare, and TRACE and EIT 195 Å intensities of the four dimmings, are plotted and compared with the GOES-8 1 – 8 Å soft X-ray flux and the CME height–time (H–T) measurements. The extrapolated CME onset time obtained by the use of a second-order polynomial fitting, and the average speed and acceleration of the CME fronts are also indicated. When the Hα and 195 Å flare light curves are approximately similar to the GOES flux profile, it is clear that the 195 Å intensities in the four dimmings obviously decreased just after the flare start time, and then these decreases continued and persisted through the extrapolated CME onset time at 07:10 UT, indicating a tight relationship among the flare, the dimmings, and the CME. Note that no brightening signal appears in the D4 intensity profile, and a point on the H–T curve of the eruptive loop system from the 07:13 UT EIT image is consistent with the extrapolated CME height curves.

To show the pre-eruption magnetic configuration and its relationship with the dimming formation, we computed a potential-field extrapolation, applying the PFSS software package available in SolarSoftWare based on synoptic magnetic maps from MDI with a 6 h time cadence (see Schrijver and DeRosa (2003) for details of the procedure). We used the synoptic map at 06:04 UT on 17 September 2002 that is closest in time to the flare studied here; representative coronal magnetic field lines in association with the dimmings are shown in

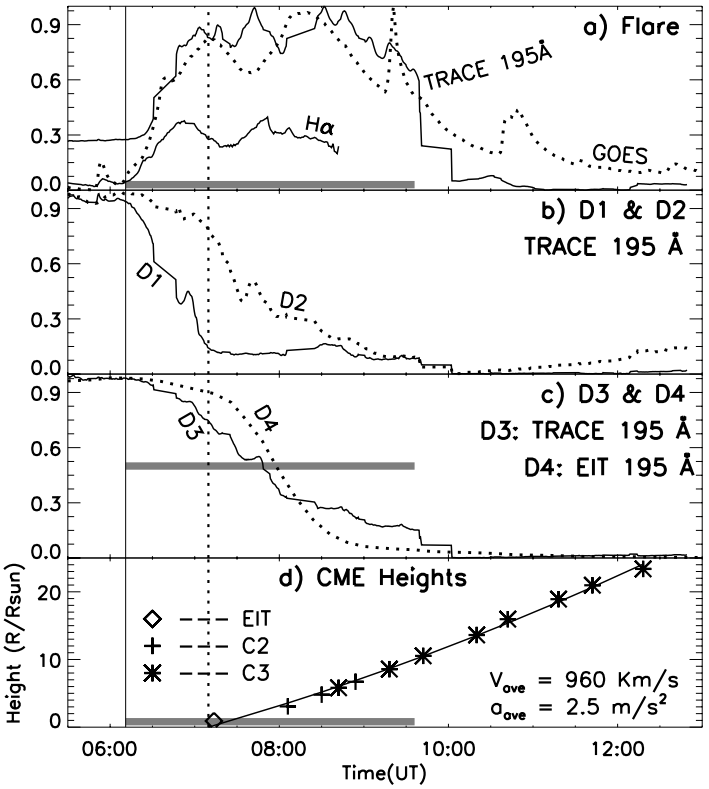

Figure 3 (a) Time profiles of GOES-8 1 – 8 Å soft X-ray flux (dashed line), YNAO Hα center (thin solid line), and TRACE 195 Å (thick solid line) flare light curves as a function of time in an area centered on the flare (indicated by the black box in Figure 1). (b, c) The light curves of TRACE and EIT 195 Å intensities in areas centered on D1 – D4 (indicated by the solid white boxes in Figures 1 and 2). The light curves are computed from the intensity integrated and normalized over these regions. (d) Heights of the CME fronts as a function of time, and the back extrapolations by the use of second-order polynomial fitting. The vertical solid bars indicate the start time of the flare, the dashed bars indicate the extrapolated onset time of the CME, and the horizontal bars indicate the duration of the flare.

Figure 4, along with superposed outlines of PIL (black) and D1 – D3 (red), and the CME direction and PIL radial direction (pink). The extrapolation clearly exhibits two different groups of magnetic loop systems, a confined one, L1 (green), and a more extended one, L2 (orange). L1 straddles PIL with opposite polarity footpoints close to or above D1 and D2, while L2 is emanated from the diffuse positive polarity D4 region well beyond AR10114 and terminated in the compact negative polarity D3 region within the region. Consistent with the EIT observations presented in Figure 2, the CME is far offset from L1 but is directed to the highest part of the long loop L2. Therefore, the extrapolation gives clear evidence that L2 is just the pre-eruptive manifestation of the eruptive huge EUV loop system and D4 indicates its distant evacuated footpoint. Since regions D1 – D4 are located around the four feet of L1 and L2, it appears that (D1, D2) and (D3, D4) are formed in pairs resulting from the eruptions of L1 and L2, respectively. As suggested by Jiang *et al.* (2009a), we can call them "quadrupolar dimmings."

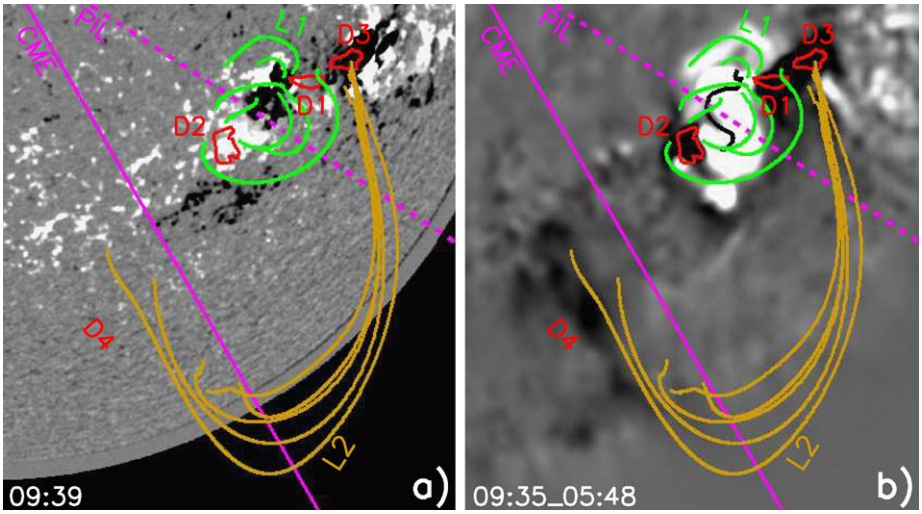

Figure 4 Overlay of MDI magnetogram (a) and EIT 195 Å base difference image (b) with the extrapolated field lines, emphasizing the magnetic connectivity of D1 – D4. The outlines of PIL (black) and D1 – D4 (red) are overlaid, and the PIL radial direction and the final CME direction are also indicated (pink). Two distinct loop systems, L1 (green) and L2 (orange), are anchored around the four dimmings. The FOV is $840'' \times 940''$.

4. Conclusions and Discussion

Though the filament did not erupt, the flare was accompanied by the formation of four obviously separate dimmings. D1 and D2, immediately adjacent to the PIL ends, probably consisted of a pair of BDDs due to an upward eruption of a flux rope in the highly sheared flare core field, while the compact D3 and the remote diffuse D4, located in the opposite polarity footpoint regions of the eruptive huge loop system, probably resulted from an expansion of this loop system simply forced by the flare field since no signature of magnetic reconnection between them was found. Nevertheless, the associated CME, laterally far offset from the flare site but almost along the eruption of the huge loops, was an over-and-out one, in which the huge loops might play a role in guiding the CME. The dimming observations are in excellent agreement with the derived PFSS magnetic configuration: the four dimmings are located around the opposite polarity footpoint regions of two loop systems. We thus conclude that regions (D1, D2) and (D3, D4) paired up in the event and formed quadrupolar dimmings.

Our event clearly illustrates that, in a single CME event, dimmings can be formed in pairs by expansion and eruption of different magnetic loop systems, and so indicate their evacuated footpoints. This implies that, based on the particular large-scale magnetic field configuration involved in the CME process, some magnetic loop systems can participate in the CME eruption and it is possible to identify the opposite polarity counterpart for a definite dimming. Our example confirms previous results that remote dimmings can be magnetically connected to a small-scale initiation region by an overlying large-scale loop system (Manoharan *et al.*, 1996). Moreover, our observations are also consistent with the magnetic-arch-blowout scenario for over-and-out CMEs proposed by Bemporad *et al.* (2005) and Moore and Sterling (2007), in which large-scale loops can laterally deflect the initial eruption and affect the final propagation direction of the CME. However, there is a difference between our event and eruptions observed by some other workers: the overlying magnetic

loops in our event might be simply pushed out by the eruptive core field rather than reconnecting with it; thus, the formation of the remote dimming is not needed to involve reconnection between the expanding CME field and surrounding small-scale loops, as described by Attrill *et al.* (2007) in their new CME evolution model. This difference seems to be due to the different orientation of the magnetic polarities of the erupting regions. For example, Attrill *et al.* (2007) in their Figure 4 showed a "positive-negative-positive-negative" field configuration in the photosphere, which is prone to reconnection of the erupting coronal loops rooted in these fields. However, the main loops in our event are rooted in photospheric fields where the strongest components form a "negative-negative-positive-positive" orientation (see Figure 4). Therefore, the loops emanating from those photospheric fields (the orange and green loops of Figure 4) do not have a configuration that is favorable for reconnection upon eruption. Probably this is why there is no (or very little) reconnection among the fields, as opposed to the events mentioned above. In this sense, our event is compatible with the recent result of Delannée (2009), and the CME became large-scale by nature rather than nurture (van Driel-Gesztelyi *et al.*, 2008).

Acknowledgements We thank an anonymous referee for valuable comments and constructive suggestions, which improved the quality of this paper. We are grateful to the observing staff at YNAO for their good-quality observations. We thank the GOES team, the TRACE team, and the SOHO/EIT, LASCO, and MDI teams for data support. This work is supported by the 973 Program (2011CB811400), by the Natural Science Foundation of China under grants 10973038 and 40636031, and by the Scientific Application Foundation of Yunnan Province under grants 2007A112M and 2007A115M.

References

Attrill, G., Harra, L.K., van Driel-Gesztelyi, L., Démoulin, P.: 2007, *Astrophys. J. Lett.* **656**, 101.
Bemporad, A., Sterling, A.C., Moore, R.L., Poletto, G.: 2005, *Astrophys. J. Lett.* **635**, 189.
Brueckner, G.E., Howard, R.A., Koomen, M.J., Korendyke, C.M., Michels, D.J., Moses, J.D., *et al.*: 1995, *Solar Phys.* **162**, 357.
Chertok, I.M., Grechnev, V.N.: 2005, *Solar Phys.* **229**, 95.
Delaboudinière, J.-P., Artzner, G.E., Brunaud, J., Gabriel, A.H., Hochedez, J.F., Millier, F., *et al.*: 1995, *Solar Phys.* **162**, 291.
Delannée, C.: 2009, *Astron. Astrophys.* **495**, 571.
Delannée, C., Hochedez, J.-F., Aulanier, G.: 2007, *Astron. Astrophys.* **465**, 603.
Handy, B.N., Acton, L.W., Kankelborg, C.C., Wolfson, C.J., Akin, D.J., Bruner, M.E., *et al.*: 1999, *Solar Phys.* **187**, 229.
Harrison, R.A.: 1986, *Astron. Astrophys.* **162**, 283.
Hudson, H.S., Cliver, E.W.: 2001, *J. Geophys. Res.* **106**, 25199.
Jiang, Y., Yang, L., Li, K., Shen, Y.: 2007, *Astrophys. J. Lett.* **662**, 131.
Jiang, Y., Bi, Y., Yang, J., Zheng, R., Wang, J.: 2009a, *Res. Astron. Astrophys.* **9**, 603.
Jiang, Y., Yang, J., Zheng, R., Bi, Y., Yang, X.: 2009b, *Astrophys. J.* **693**, 1851.
Liu, C., Lee, J., Deng, N., Gary, D.E., Wang, H.: 2006, *Astrophys. J.* **642**, 1205.
Mandrini, C.H., Nakwacki, M.S., Attrill, G., van Driel-Gesztelyi, L., Démoulin, P., Dasso, S., Elliott, H.: 2007, *Solar Phys.* **244**, 25.
Manoharan, P.K., van Driel-Gesztelyi, L., Pick, M., Démoulin, P.: 1996, *Astrophys. J. Lett.* **468**, 73.
Moore, R.L., Sterling, A.C.: 2007, *Astrophys. J.* **661**, 543.
Pevtsov, A.A.: 2002, *Solar Phys.* **207**, 111.
Scherrer, P.H., Bogart, R.S., Bush, R.I., Hoeksema, J.T., Kosovichev, A.G., Schou, J., *et al.*: 1995, *Solar Phys.* **162**, 129.
Schrijver, C.J., DeRosa, M.L.: 2003, *Solar Phys.* **212**, 165.
Steinegger, M., Denker, C., Goode, P.R., Marquette, W.H., Varsik, J., Wang, H., *et al.*: 2000, In: Wilson, A. (ed.) *The Solar Cycle and Terrestrial Climate*, *ESA-SP 463*, 617.
Sterling, A.C., Hudson, H.S.: 1997, *Astrophys. J. Lett.* **491**, 55.
van Driel-Gesztelyi, L., Attrill, G., Démoulin, P., Mandrini, C.H., Harra, L.K.: 2008, *Ann. Geophys.* **26**, 3077.

Wang, H., Qiu, J., Jing, J., Spirock, T.J., Yurchyshyn, V., Abramenko, V., Ji, H., Goode, P.R.: 2004, *Astrophys. J.* **605**, 931.
Wang, T., Yan, Y., Wang, J., Kurokawa, H., Shibata, K.: 2002, *Astrophys. J.* **572**, 580.
Webb, D.F., Lepping, R.P., Burlaga, L.F., DeForest, C.E., Larson, D.E., Martin, S.F., Plunkett, S.P., Rust, D.M.: 2000, *J. Geophys. Res.* **105**, 27251.
Zhang, Y., Wang, J., Attrill, G., Harra, L.K., Yang, Z., He, X.: 2007, *Solar Phys.* **241**, 329.
Zhukov, A.N., Veselovsky, I.S.: 2007, *Astrophys. J. Lett.* **664**, 131.